J Therm Anal Calorim (2010) 100:607–614
DOI 10.1007/s10973-009-0592-4

Comparisons of *n*th-order kinetic algorithms and kinetic model simulation on HMX by DSC tests

Chun-Ping Lin · Yi-Ming Chang · Jo-Ming Tseng · Chi-Min Shu

Received: 9 April 2009 / Accepted: 28 October 2009 / Published online: 10 December 2009

Abstract Octahydro-1,3,5,7-tetranitro-1,3,5,7-tetrazocine (HMX) is a typical highly energetic material that has been widely used in national defense industries since the 1940s. The aim of this study was to establish a reaction kinetic model on thermal decomposition properties via differential scanning calorimetry (DSC) by well-known kinetic equations and kinetic model simulation. Furthermore, the aim also was to compare kinetic algorithms for thermal decomposition energy parameters under various conditions. Experimental results highly depended on the reliability of the kinetic concept applied, which is essentially defined by the proper choice of a mathematical model of a reaction. In addition, the correctness of the methods is used for kinetics evaluation.

Keywords Differential scanning calorimetry (DSC) · Energetic material · Kinetic algorithms · Kinetic · Model simulation · Octahydro-1,3,5,7-tetranitro-1,3,5,7-tetrazocine (HMX)

C.-P. Lin · Y.-M. Chang · C.-M. Shu
Graduate School of Engineering Science and Technology, National Yunlin University of Science and Technology (NYUST), 123, University Rd., Sec. 3, Douliou, Yunlin 64002, Taiwan, ROC

J.-M. Tseng
Institute of Safety and Disaster Prevention Technology, Central Taiwan University of Science and Technology, 666, Buzih Rd., Beitun District, Taichung 40601, Taiwan, ROC

C.-M. Shu (✉)
Department of Safety, Health, and Environmental Engineering, NYUST, 123, University Rd., Sec. 3, Douliou, Yunlin 64002, Taiwan, ROC
e-mail: shucm@yuntech.edu.tw

List of symbols

*N*th-order kinetic algorithm

A	Pre-exponential factor (s^{-1})
E_a	Activation energy (kJ mol^{-1})
$E_{\alpha i}$	Activation energy at isoconversional degree α_i (kJ mol^{-1}), $i = 1, 2, 3, 4$
$f(\alpha)$	Kinetic functions
K	Heat conduction coefficient (W m^{-1} K^{-1})
Q	Total heat of reaction (kJ kg^{-1})
R	Gas constant, 8.31415 (J K^{-1} mol^{-1})
T_0	Exothermic onset temperature (°C)
T_f	Final temperature (°C)
T_P	Peak temperature (°C)
T_{Pi}	Peak temperature of different scanning rates (°C), $i = 1, 2, 3, 4$
$T_{\alpha i}$	Different temperature in various scanning rates at isoconversional degree α_i, $i = 1, 2, 3, 4$
A	Degree of conversion, dimensionless
βi	Scanning rate (°C min^{-1}), $i = 1, 2, 3, 4$
ΔH_d	Heat of decomposition (kJ kg^{-1})

Kinetic model simulations

E_1	Activation energy of 1st stage (kJ mol^{-1})
E_2	Activation energy of 2nd stage (kJ mol^{-1})
E_a	Activation energy (kJ mol^{-1})
f_i	Kinetic functions of ith stage, $i = 1, 2, 3$
k_0	Pre-exponential factor (m^3 mol^{-1} s^{-1})
k_i	Rate constant of ith stage (mol L^{-1} s^{-1}), $i = 1, 2, 3$
n_i	Reaction order of ith stage, dimensionless, $i = 1, 2, 3$
Q_0	Heat production (kJ kg^{-1})
Q_t	Heat production rate (kJ kg^{-1} min^{-1})
r_i	Reaction rate of ith stage (g s^{-1}), $i = 1, 2, 3, 4$
T	Absolute temperature (K)
T	Time (s)
Z	Autocatalytic constant, dimensionless

A Degree of conversion, dimensionless
α_i Reaction order of ith stage, dimensionless; $i = 1, 2, 3, 4$
γ Degree of conversion, dimensionless

Introduction

Octahydro-1,3,5,7-tetranitro-1,3,5,7-tetrazocine (HMX) is widely employed as a compound material with other energetic materials or single use, applied on military dynamite during manufacturing in various countries. The thermal decomposition energy (activation energy, E_a) for HMX was investigated by differential scanning calorimetry (DSC) [1]. Comparisons of activation energy for HMX at different scanning rates (1, 2, 4, and 10 °C min^{-1}) tested by DSC were also discussed in this study.

Furthermore, aim of this study was to evaluate thermal experimental data of HMX via DSC, by applying well-known kinetic equations such as the Kissinger kinetic equation [2], Augis–Bennett kinetic equation [3], and Ozawa–Flynn–Wall kinetic equation [4–8] in various scanning rates, and then to compare thermal safety software (TSS) for kinetics evaluation [9–11]. This was along with a comparison of the mathematical [12–15] and simulation approaches to develop a precise and effective procedure on thermal decomposition properties for HMX.

Comparisons of an *n*th-order kinetic algorithm and kinetic model simulation can be used for many important purposes, such as conceptual design and optimization of chemical processes, reactor design, assessment of reaction hazards, choice of safe conditions of storage and transportation of a commercial chemical, etc. [16–21].

Experimental and methods

Differential scanning calorimetry

Samples of HMX were supplied directly by National Defense University of the Republic of China (ROC). Non-isothermal DCS analysis of the samples was conducted on a Mettler TA8000 system; scanning rates chosen for the temperature programmed ramp were 1, 2, 4, and 10 °C min^{-1} (sample mass ≈ 1.4 mg; no carrier gas was applied in thermal degradation condition). STAR^e software was employed to obtain thermal curves [1]. DSC analysis on the samples sealed in 40 μL aluminum pans was carried out via a Mettler ME-27311 DSC instrument in a crucible with a lid having small (pin size) hole in the center. The range of temperature rise was selected from 30 to 300 °C for each experiment.

*N*th-order kinetic algorithm

The Kissinger kinetic equation, Augis–Bennett kinetic equation, and Ozawa–Flynn–Wall kinetic equation in various scanning rates (1, 2, 4, and 10 °C min^{-1}) were individually adopted to evaluate HMX's thermokinetic parameters [2–8].

Kinetic model simulations

Processing of experimental data and kinetics evaluation were implemented by applying TSS developed by Chem-Inform Saint-Petersburg (CISP) Ltd. The method is thoroughly described by Kossoy, Benin, and Akhmetshin for the creation of a kinetic model and the algorithms that were adopted [9–11].

Results and discussion

*N*th-order kinetic algorithm

Kissinger kinetic equation

Kissinger's formal model can represent on the basis of scanning rate and peak temperature that may consist of several dependent equations as illustrated below [2].

$$\ln\left(\frac{\beta}{T_P^2}\right) = \ln\frac{AR}{E_a} - \frac{E_a}{RT_P} \quad (1)$$

where β is the scanning rate, T_P is the peak temperature, A is the pre-exponential factor, E_a is the activation energy, and R is the gas constant.

DSC thermal curves for HMX decomposition with scanning rates 1, 2, 4, and 10 °C min^{-1} are displayed in Fig. 1. The E_a of thermal decomposition was calculated by our experimental data from DSC tests as listed in Table 1. The activation energy analysis graphs for HMX with different scanning rates of 1, 2, 4, and 10 °C min^{-1} by Kissinger kinetic equation are in Fig. 2. The E_a calculated by the kinetic equation was 238 kJ mol^{-1}.

Augis–Bennett kinetic equation

According to the method suggested by Augis and Bennett [3],

$$\ln\left(\frac{\beta}{T_P - T_0}\right) = \ln A - \frac{E_a}{RT_P} \quad (2)$$

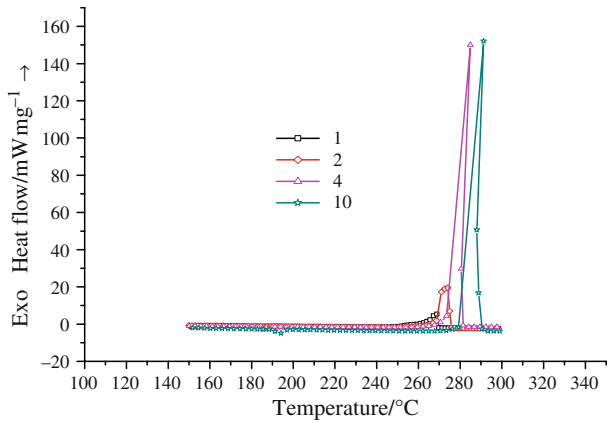

Fig. 1 DSC thermal curves for HMX decomposition with scanning rates of 1, 2, 4, and 10 °C min^{-1}

Table 1 Experimental data for HMX's thermal decompositions via STAR^{e} software by DSC tests

Sample scanning rate/°C min^{-1}	HMX			
	1	2	4	10
T_0/°C	241.77	247.67	257.27	267.27
T_P/°C	268.81	274.15	284.91	288.05
T_f/°C	271.88	276.98	282.43	293.35
ΔH_d/kJ kg^{-1}	2076.60	2011.90	1907.75	1896.15

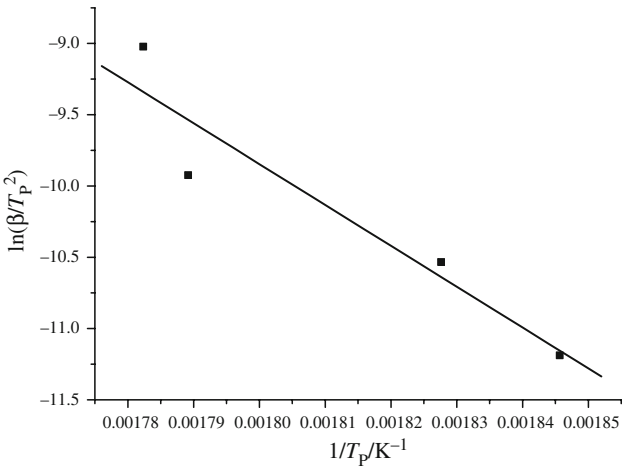

Fig. 2 Activation energy analysis graph for HMX with scanning rates of 1, 2, 4, and 10 °C min^{-1} by Kissinger kinetic equation

where T_p and T_0 are the peak temperature and the onset temperature of the DSC peak, respectively. The E_a can be obtained from the slope of the straight line $\ln[\beta/(T_p - T_0)^{-1}]$ vs. T_p^{-1} [3].

DSC experimental data were processed by applying the kinetic equation, this reaction kinetic model based upon heat of decomposition, onset temperature, peak temperature, and scanning rate [6]. The activation energy analysis graphs for HMX with scanning rates of 1, 2, 4, and 10 °C min^{-1} are shown in Fig. 3. The E_a value computed by the kinetic equation was 279 kJ mol^{-1}, and then the combined Kissinger's method of thermokinetic parameters is listed in Table 2.

Ozawa–Flynn–Wall kinetic equation

A formal model can represent the reaction excursion based upon a scanning rate that may consist of several dependent equations as illustrated below [4–8]:

$$\ln(\beta) = -1.0516\frac{E_a}{RT} + \text{const.} \tag{3}$$

At different scanning rates under isoconversional degree condition, a set of kinetic equations can be derived [4–8]:

$$\ln\beta_1 + \frac{1.0516E_{ai}}{RT_{\alpha 1}} = \ln\beta_2 + \frac{1.0516E_{ai}}{RT_{\alpha 2}} = \ln\beta_3 + \frac{1.0516E_{ai}}{RT_{\alpha 3}} = \ln\beta_4 + \frac{1.0516E_{ai}}{RT_{\alpha 4}} = \cdots \tag{4}$$

where β_1, β_2, β_3, and β_4 are different scanning rates; E_{ai} is the activation energy at isoconversional degree αi; $T_{\alpha 1}$, $T_{\alpha 2}$, $T_{\alpha 3}$, and $T_{\alpha 4}$ are different temperatures in various scanning rates at isoconversional degree αi.

The activation energy analysis graphs for HMX with scanning rates of 1, 2, 4, and 10 °C under isoconversional degree at 1, 5, 10, 15, 20, and 25% (the degree of conversion more than 25% are unstable via scanning rates 4 and 10 °C min^{-1} condition) by kinetic equation are illustrated in Fig. 4; the thermokinetic parameters of thermal decomposition are given in Table 3.

We acquired thermokinetic parameters for thermal decomposition properties by the above-mentioned

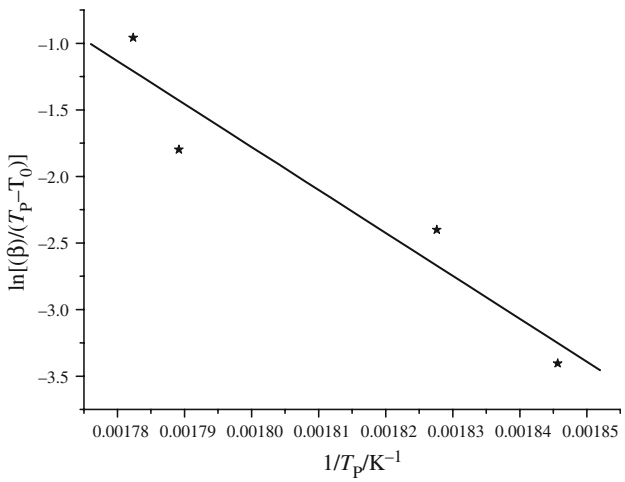

Fig. 3 Activation energy analysis graph for HMX with scanning rates of 1, 2, 4, and 10 °C min^{-1} by Augis–Bennett kinetic equation

Table 2 Results of thermokinetic parameters for the thermal decompositions of HMX at T_P by Kissinger and Augis–Bennett kinetic equations

Sample kinetic model	HMX		
	Activation energy, E_a/kJ mol^{-1}	Correlation coefficient, R^2	Standard deviation
Kissinger	238.34	0.89634	0.36304
Augis–Bennett	279.45	0.93369	0.38386

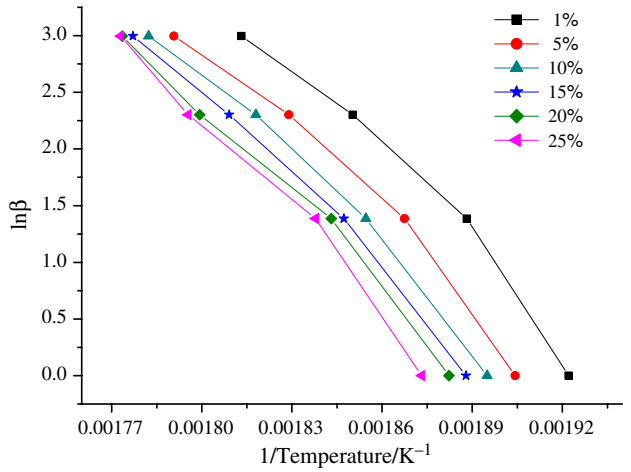

Fig. 4 Activation energy analysis graphs for HMX with scanning rates of 1, 2, 4, and 10 °C min^{-1} under isoconversional degree at 1, 5, 10, 15, 20, and 25% by Ozawa–Flynn–Wall kinetic equation

approaches. The thermokinetic parameters for the thermal decompositions of HMX are presented in Tables 2 and 3. We compared with the E_a of thermal decomposition in the literature displayed in Table 4 [12–15], HMX ca. 130–450 kJ mol^{-1}. In contrast to Tables 2–4, HMX's E_a value is in the uncertain range ca. 130–450 kJ mol^{-1} which would be confusing.

Therefore, well-known kinetic equations provided a swift mathematical model for analyzing HMX's E_a. In fact, we should first be alert to the accuracy problem. From Fig. 1, we can see that the greater the scanning rate, the worse the stability and applicability of HMX. This because the greater the scanning rate might generate, the wider and smoother thermal analysis curve from neglecting the slight thermal decomposition differences. In addition, from Fig. 5, for DSC via the smaller scanning rate at 1 and 2 °C min^{-1}, the degree of conversion is stable, but a greater scanning rate at scanning rate at 4 and 10 °C min^{-1} would be overheating of the sample. From Table 2, we took a look at Lee et al. [13] and Chovancová and Zeman [15] via various heating rates at 5, 10, 15, and 20 °C min^{-1} and 5, 10, and 15 °C min^{-1} by DSC and DTA, respectively. Thus, we hypothesized, that the error came from overheating of the sample, to create the E_a value in the uncertain range.

Kinetic model simulations

Determination of HMX's thermokinetic parameters by simulation

Formal models can represent complex multi-stage reactions that may consist of several independent, parallel, and consecutive stages, as illustrated by the following patterns [9–11].

The initial conditions were as follows:

$$\frac{d\alpha_1}{dt} = r_1 = k_1(T)f_1$$

$$\frac{d\alpha_2}{dt} = r_1 - r_2; \quad r_2 = k_2(T)f_2$$

$$\frac{d\alpha_3}{dt} = r_2 - r_3; \quad r_3 = k_3(T)f_3$$

$$\frac{d\alpha_4}{dt} = r_3$$

$$t = 0; \quad \alpha_i = 0; \quad i = 1,\ 2,\ 3,\ 4 \qquad (5)$$

where α_1, α_2, α_3, and α_4 are the conversion of a reaction or stage; r_1, r_2, and r_3 are reaction rates of a reaction or stage;

Table 3 HMX's thermokinetic parameters for the thermal decompositions in various degree of conversions 1, 5, 10, 15, 20, and 25% by Ozawa–Flynn–Wall kinetic equation

Sample degree of conversion, α/%	HMX		
	Activation energy, E_a/kJ mol^{-1}	Correlation coefficient, R^2	Standard deviation
1	214.08	0.96851	0.28137
5	206.15	0.97265	0.26220
10	211.70	0.98355	0.20331
15	212.23	0.98835	0.17111
20	211.80	0.98726	0.17888.
25	227.82	0.98430	0.19870
Average	213.96	N/A	N/A

Table 4 Comparisons of E_a for HMX in the literature [12–15]

Authors	Activation energy, E_a/kJ mol^{-1}	Year	Method
Vyazovkin and Wight [12]	ca. 140	1999	Model fitting and model free under non-isothermal (in various heating rates at 0.17, 0.34, 0.51, and 0.68 °C min^{-1}) and isothermal condition (hold on temperature at 230, 235, 240, 245, and 250 °C) by TGA
Lee et al. [13]	444	2002	Kissinger's method by DSC (in various scanning rates at 5, 10, 15, and 20 °C min^{-1})
Singh et al. [14]	ca. 196–204	2003	Arrhenius parameters evaluated by TGA under isothermal condition (hold on temperature at 265, 267, 270, 275, and 280 °C)
Chovancová and Zeman [15]	220.5	2007	Kissinger's method by DTA (in various heating rates at 5, 10, and 15 °C min^{-1})

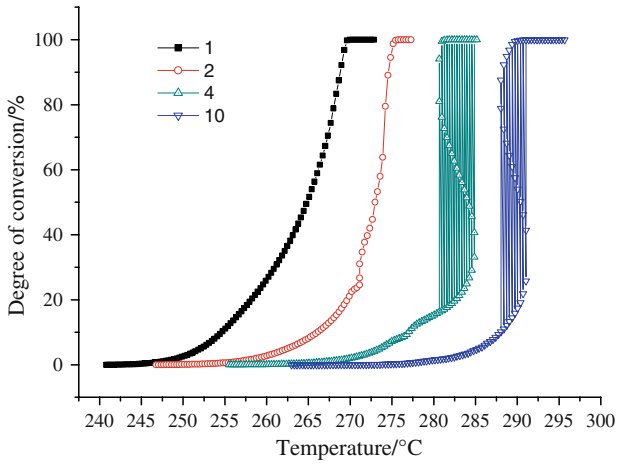

Fig. 5 HMX's α versus temperature curves with scanning rates of 1, 2, 4, and 10 °C min^{-1} by DSC tests

k_1, k_2, and k_3 are the rate constants of a reaction or stage; f_1, f_2, and f_3 are the kinetic functions of a reaction or stage.

Simple single-stage reaction $A \rightarrow B$:

$$\frac{d\alpha}{dt} = k_0 e^{-\frac{E_a}{RT}} f(\alpha) \tag{6}$$

$$f(\alpha) = (1-\alpha)^n \quad N\text{th - order}$$

$$f(\alpha) = (1-\alpha)^{n_1}(\alpha^{n_2} + z) \quad \text{Autocatalytic}$$

where E_a is the activation energy, k_0 is the pre-exponential factor, z is the autocatalytic constant, n_1 and n_2 are reaction orders of a specific stage.

Reaction includes two consecutive stages: $A \rightarrow B \rightarrow C$:

$$\frac{d\alpha}{dt} = k_1 e^{-\frac{E_1}{RT}}(1-\alpha)^{n_1}; \quad \frac{d\gamma}{dt} = k_2 e^{-\frac{E_2}{RT}}(\alpha-\gamma)^{n_2} \tag{7}$$

where α and γ are conversions of the reactant A and product C, respectively, and E_1 and E_2 are activation energies of stages 1 and 2.

Two-parallel reactions are very useful models of full autocatalysis:

$$\frac{d\alpha}{dt} = r_1(\alpha) + r_2(\alpha); \quad \begin{matrix} r_1(\alpha) = k_1(T)(1-\alpha)^{n_1} \\ r_2(\alpha) = k_2(T)\alpha^{n_2}(1-\alpha)^{n_3} \end{matrix} \tag{8}$$

where r_1 and r_2 are rates of stages 1 and 2, and n_3 is reaction order of stage 3.

The kinetic evaluation parameters were computed by our experimental data from DSC tests. In particular, we hypothesized HMX's thermal decomposition belonged to an unknown reaction, such as *n*th-order or autocatalytic

Table 5 HMX's thermokinetic parameters evaluated by *n*th-order and autocatalytic simulation

Sample scanning rate/°C min^{-1}	HMX							
	*N*th-order				Autocatalytic			
	1	2	4	10	1	2	4	10
ln(k_0)/ln/s^{-1}	69.49	106.36	38.85	39.65	24.20	26.47	23.58	24.70
Activation energy, E_a/kJ mol^{-1}	340.71	507.0366	199.81	203.23	135.32	137.98	117.81	123.42
Reaction order, *n*/*n*th reaction order, n_1/auto	3.000E-08	1.527E-06	0.0988	0.0243	0.1282	0.8044	1.3058	0.8132
Reaction order, n_2	N/A	N/A	N/A	N/A	0.8739	0.8825	1.5373	1.2059
Autocatalytic constant, z	N/A	N/A	N/A	N/A	0.0333	8.437E-05	3.733E-04	1.556E-04
ΔH_d/kJ kg^{-1}	2115.58	2276.04	2388.72	2052.28	2151.73	2258.87	2503.23	2112.01

Table 6 HMX's TMR, TER, and TCL at scanning rates of 1, 2, 4, and 10 °C min^{-1} by *n*th-order simulation

Sample scanning rate		HMX										
		1 °C min^{-1}			2 °C min^{-1}			4 °C min^{-1}			10 °C min^{-1}		
Item no.	Temperature/ °C	TMR/ min	TER/ kJ kg^{-1}	TCL/day (CL = 10%)	TMR/ min	TER/ kJ kg^{-1}	TCL/day (CL = 10%)	TMR/ min	TER/ kJ kg^{-1}	TCL/day (CL = 10%)	TMR/ min	TER/ kJ kg^{-1}	TCL/day (CL = 10%)
1	20	0	5.42E-21	3652.5	N/A	N/A	N/A	0	3.85E-09	3652.5	0	2.00E + 01	3652.5
2	27.27	0	1.60E-19	3652.5	N/A	N/A	N/A	0	2.80E-08	3652.5	0	2.73E + 01	3652.5
3	34.55	0	4.02E-18	3652.5	N/A	N/A	N/A	0	1.86E-07	3652.5	0	3.46E + 01	3652.5
4	41.82	0	8.69E-17	3652.5	N/A	N/A	N/A	144000	1.13E-06	3652.5	0	4.18E + 01	3652.5
5	49.09	0	1.64E-15	3652.5	N/A	N/A	N/A	144000	6.30E-06	3652.5	144000	4.91E + 01	3652.5
6	56.36	0	2.71E-14	3652.5	N/A	N/A	N/A	144000	3.27E-05	3652.5	144000	5.64E + 01	3652.5
7	63.64	0	3.98E-13	3652.5	N/A	N/A	N/A	144000	1.58E-04	3652.5	144000	6.36E + 01	3652.5
8	70.91	0	5.21E-12	3652.5	N/A	N/A	N/A	144000	7.13E-04	3652.5	144000	7.09E + 01	3652.5
9	78.18	0	6.13E-11	3652.5	N/A	N/A	N/A	144000	3.03E-03	3652.5	144000	7.82E + 01	3652.5
10	85.45	0	6.53E-10	3652.5	N/A	N/A	N/A	144000	1.21E-02	3652.5	144000	8.55E + 01	3652.5
11	92.73	0	6.33E-09	3652.5	N/A	N/A	N/A	144000	4.60E-02	3652.5	144000	9.27E + 01	3652.5
12	100	0	5.61E-08	3652.5	N/A	N/A	N/A	144000	1.67E-01	3652.5	144000	1.00E + 02	3652.5

Table 7 HMX's TMR, TER, and TCL at scanning rates of 1, 2, 4, and 10 °C min^{-1} by autocatalytic simulation

Sample scanning rate		HMX										
		1 °C min^{-1}			2 °C min^{-1}			4 °C min^{-1}			10 °C min^{-1}		
Item no.	Temperature/ °C	TMR/ min	TER/ kJ kg^{-1}	TCL/day (CL = 10%)	TMR/ min	TER/ kJ kg^{-1}	TCL/day (CL = 10%)	TMR/ min	TER/ kJ kg^{-1}	TCL/day (CL = 10%)	TMR/ min	TER/ kJ kg^{-1}	TCL/day (CL = 10%)
1	20	144000	1.55E-05	3652.5	144000	1.34E-07	3652.5	144000	1.43E-04	3652.5	144000	1.54E-05	3652.5
2	27.27	144000	5.96E-05	3652.5	144000	5.28E-07	3652.5	144000	4.60E-04	3652.5	144000	5.25E-05	3652.5
3	34.55	144000	2.15E-04	3652.5	144000	1.95E-06	3652.5	144000	1.40E-03	3652.5	144000	1.69E-04	3652.5
4	41.82	144000	7.27E-04	3652.5	144000	6.78E-06	3652.5	144000	4.06E-03	3652.5	144000	5.14E-04	3652.5
5	49.09	144000	2.34E-03	3652.5	144000	2.23E-05	3652.5	144000	1.12E-02	3652.5	144000	1.49E-03	3652.5
6	56.36	144000	7.13E-03	3652.5	144000	6.95E-05	3652.5	144000	2.96E-02	3652.5	144000	4.12E-03	3652.5
7	63.64	144000	2.07E-02	3652.5	144000	2.07E-04	3652.5	144000	7.50E-02	3652.5	144000	1.09E-02	3652.5
8	70.91	144000	5.78E-02	3652.5	144000	5.94E-04	3652.5	144000	1.83E-01	3652.5	144000	2.79E-02	3652.5
9	78.18	144000	1.55E-01	3652.5	144000	1.65E-03	3652.5	144000	4.33E-01	3652.5	144000	6.91E-02	3652.5
10	85.45	144000	4.00E-01	3652.5	144000	4.58E-03	3652.5	144000	1.00E + 00	2949.47	144000	1.66E-01	3137.83
11	92.73	144000	1.02E + 00	3652.5	144000	1.24E-02	3652.5	144000	2.30E + 00	1344.77	144000	4.01E-01	1378.09
12	100	144000	2.58E + 00	3579.8	144000	3.40E-02	3086.57	144000	5.59E + 00	632.19	144000	1.04E + 00	624.96

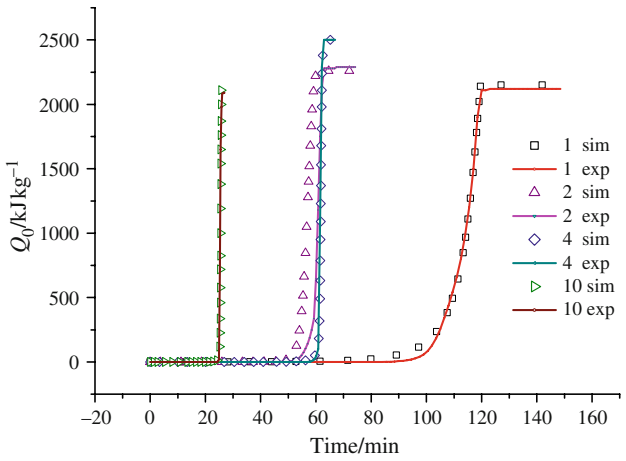

Fig. 6 Comparisons of HMX's Q_0 versus time curves of autocatalytic reaction with scanning rates of 1, 2, 4, and 10 °C min^{-1} by simulation and experiment

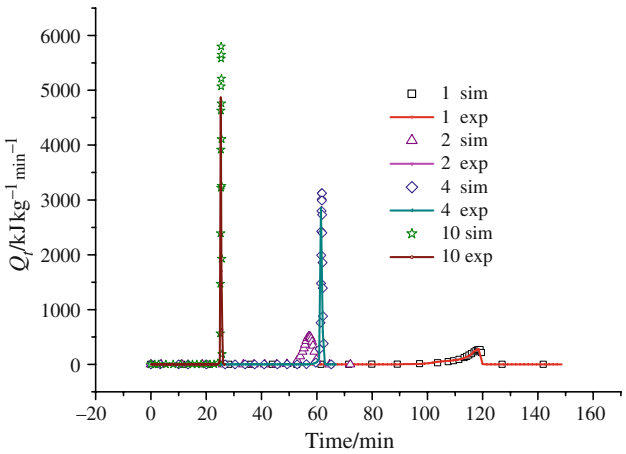

Fig. 7 Comparisons of HMX's Q_t versus time curves of autocatalytic reaction with scanning rates of 1, 2, 4, and 10 °C min^{-1} by simulation and experiment

reaction. We tried to employ *n*th-order and autocatalytic simulation to compute thermokinetic parameters. The two condition simulation results of thermokinetic parameters were evaluated as given in Table 5. Meanwhile, the time to maximum rate (TMR), the total energy release (TER), and the time to conversion limit (TCL) of HMX were obtained in various scanning rates as shown in Tables 6 and 7.

In contrast to Tables 5–7, we could observe the results of an *n*th-order reaction kinetic simulation and autocatalytic reaction kinetic simulation for HMX, in which thermokinetic parameters were providing the results disorderly and confused by *n*th-order reaction simulation. The result is explicit: the *n*th-order reaction simulation is not appropriately applied on HMX's thermokinetic parameter evaluation. Comparisons of autocatalytic reaction of simulation and experiment for heat production (Q_0) versus time and heat production rate (Q_t) versus time are illustrated in Figs. 6 and 7, respectively.

Well-known kinetic equations and simulation approach were based upon *n*th-order kinetic algorithms and kinetic model simulation, respectively. In fact, we should also concern ourselves with the accuracy problem for the simulation model. From Table 7, we observed that a greater scanning rate of more than 2 °C min^{-1}, the lesser the stability of thermal decomposition phenomenon is demonstrated for the kinetic parameters. From Figs. 6 and 7, we can also see that the greater the scanning rate, the wider and smoother the thermal analysis curves and overheating of thermal decomposition again.

Furthermore, while analyzing HMX's thermokinetic parameters of thermal decomposition by DSC, we can make the following statement: for processing of *n*th-order kinetic algorithm or kinetic model simulation computing of HMX's thermokinetic parameters, we received a better result for scanning rates under a slower scanning rate such as 1 and 2 °C min^{-1}, which then also could be matched with Vyazovkin and Wight's results [12]. Therefore, while analyzing HMX's thermokinetic parameters of thermal decomposition by simulation approach, we obtained a better result at a scanning rate of 1 and 2 °C min^{-1} in this study. In addition, from Table 7, we can also obtain HMX's TMR as it is a little less than 100 °C, which exceeds the upper limit of 100 days and TCL is somewhat less than 92 °C, which exceeds the upper limit of 10 years (1 and 2 °C min^{-1}).

Conclusions

We have derived an accurate analysis model on thermokinetic parameters of HMX for thermal decomposition. In addition to analyzing an energetic material's thermal decomposition kinetic parameter through *n*th-order kinetic algorithms and kinetic model simulation, we found that the simulation presented a reasonable model for calculating an energetic material's thermal decomposition E_a. We also discovered adequate scanning rates on acquiring thermal decomposition E_a under slower scanning rate for an energetic chemical of interest. As a consequence, the validity of the results acquired significantly depends on the reliability of the kinetic model applied, which is essentially verified by the proper selection of a mathematical model of a reaction and the correctness of the methods used for the kinetic evaluation of highly energetic materials.

Acknowledgements The authors are indebted to Dr. Yao-Hsun Hung, Dr. Tzu-Wan Ho, and Dr. Chang-Ping Chang for technical suggestions on experiments and analyses of HMX thermal properties. In addition, the authors are grateful to National Defense University of ROC in Taiwan.

References

1. STAR^e Software with Solaris Operating System. Operating Instructions. Mettler Toledo. Sweden, 2004.
2. Kissinger HE. Reaction kinetics in differential thermal analysis. Anal Chem. 1957;29:1702–6.
3. Augis JA, Bennett JE. Calculation of the Avrami parameters for heterogeneous solid-state reactions using a modification of the Kissinger method. J Therm Anal. 1978;13:283–92.
4. Ozawa T. A new method of analyzing thermogravimetric data. Bull Chem Soc J. 1965;38:1881–6.
5. Ozawa T. Kinetic analysis of derivative curves in thermal analysis. J Therm Anal. 1970;2:301–24.
6. Ozawa T. Estimation of activation energy by isoconversion methods. Thermochim Acta. 1992;203:159–65.
7. Ozawa T. Thermal analysis-review and prospect. Thermochim Acta. 1999;355:35–42.
8. Flynn JH, Wall LA. A quick, direct method for the determination of activation energy from thermogravimetric data. J Polym Sci Part B. 1966;4(5):323–8.
9. Kossoy AA, Akhmetshin YG. Identification of kinetic models for the assessment of reaction hazards. Process Saf Prog. 2007;26(3):209–20.
10. Kossoy AA, Benin AI, Akhmetshin YG. An advanced approach to reactivity rating. J Hazard Mater. 2005;118(1–3):9–17.
11. Thermal Safety Software (TSS). ChemInform Saint-Petersburg (CISP) Ltd., St. Petersburg, Russia, http://www.cisp.spb.ru
12. Vyazovkin S, Wight CA. Model-free and model-fitting approaches to kinetic analysis of isothermal and nonisothermal data. Thermochim Acta. 1999;340–341:53–68.
13. Lee JS, Hsu CK, Chang CL. A study on the thermal decomposition behaviors of PETN, RDX, HNS and HMX. Thermochim Acta. 2002;392–393:173–6.
14. Singh G, Felix SP, Soni P. Studies on energetic compounds part 28: thermolysis of HMX and its plastic bonded explosives containing Estane. Thermochim Acta. 2003;399:153–65.
15. Chovancová M, Zeman S. Study of initiation reactivity of some plastic explosives by vacuum stability test and non-isothermal differential thermal analysis. Thermochim Acta. 2007;460:67–76.
16. Brown ME, Maciejewski M, Vyazovkin S, Nomen R, Sempere J, Burnham A, et al. Computational aspects of kinetic analysis part A: the ICTAC kinetics project-data, methods and results. Thermochim Acta. 2000;355:125–43.
17. Sewry JD, Brown ME. Model-free kinetic analysis? Thermochim Acta. 2002;390:217–25.
18. Tanaka H, Brown ME. The theory and practice of thermoanalytical kinetic of solid-state reactions. J Therm Anal Calorim. 2005;80:795–7.
19. Roduit B, Borgeat C, Berger B, Folly P, Andres H, Schädeli U, et al. Up-scaling of DSC data of high energetic materials simulation of cook-off experiments. J Therm Anal Calorim. 2006;85:195–202.
20. Lin CP, Shu CM. A comparison of thermal decomposition energy and nitrogen content of nitrocellulose in non-fat process of linters by DSC and EA. J Therm Anal Calorim. 2008;95:547–52.
21. Käser F, Bohn MA. Decomposition in HTPB bonded HMX followed by heat generation rate and chemiluminescence. J Therm Anal Calorim. 2009;96:687–95.